# Angular distributions for $^{16}O(\gamma,p)^{15}N$ at intermediate energies

G. S. Adams
*Department of Physics, Rensselaer Polytechnic Institute, Troy, New York 12180*

E. R. Kinney, J. L. Matthews, W. W. Sapp, and T. Soos
*Department of Physics and Laboratory for Nuclear Science, Massachusetts Institute of Technology, Cambridge, Massachusetts 02139*

R. O. Owens
*Department of Physics and Astronomy, Glasgow University, Glasgow G12, Scotland*

R. S. Turley
*Hughes Research Laboratories, Malibu, California 90265*

G. Pignault*
*Department of Physics, University of South Carolina, Columbia, South Carolina 29208*
(Received 6 June 1988)

The photoproton knockout reaction on $^{16}O$ leaving $^{15}N$ in low-lying bound states has been observed over the photon energy range from 196 to 361 MeV. The angular distribution for the reaction populating the ground state of $^{15}N$ develops sharp structure as the photon energy is increased but that for population of the excited states is smooth. The results are not explained by existing theoretical models.

## I. INTRODUCTION

Few data have been published for intermediate energy photonucleon reactions on targets heavier than $^4He$. Excitation functions have been measured at a few angles on targets of $^{16}O$ (Ref. 1), and $^{40}Ca$ (Ref. 2), while the only detailed angular distribution that has been reported is the initial result[3] at $E_\gamma = 196$ MeV of the present work on the $^{16}O(\gamma,p_0)$ reaction.

Theoretical analyses of these data have not been very successful. There seems to be agreement that the single-nucleon knock-out amplitudes alone produce too small a cross section at large values of momentum mismatch (or three-momentum transfer), $q = |\mathbf{p}-\mathbf{p}_\gamma|$, between the large final-state proton momentum $\mathbf{p}$ and relatively small initial photon momentum $\mathbf{p}_\gamma$. Models which include two-nucleon processes via intermediate $\Delta(1232)$ excitations,[4] meson exchange,[5] or phenomenological quasideuteron amplitudes,[6] do result in a cross section of more nearly the correct magnitude, but none of the published calculations is able quantitatively to reproduce the available data. Although the choice of parameters in some of the existing calculations has been questioned,[1] and the best choice is not clear, the basic problem lies in the absence of a comprehensive theoretical treatment of the exclusive $(\gamma,N)$ reaction which includes all of the important mechanisms.

Further theoretical work would be assisted by more comprehensive measurements of the $(\gamma,p)$ angular distribution over a wide range of photon energies, in order to help establish the relative importance of different reaction mechanisms. Some theoretical models predict distinctive and systematically varying structures in the angular distribution due to the interference between different mechanisms.[4,5] These models are not in good accord with the 196 MeV data on $^{16}O(\gamma,p)^{15}N$ (see Ref. 3) but comparison at a single photon energy gives little indication of the source of the discrepancy.

The results reported here are an extension of the initial experiment at $E_\gamma = 196$ MeV. They comprise angular distributions for the protons populating the ground state and low lying $^{15}N$ excited states in the $^{16}O(\gamma,p)$ reaction at photon energies of 257, 312, and 361 MeV.

## II. EXPERIMENT

The measurements were carried out at the MIT–Bates Linear Electron Accelerator. The technique was essentially the same as that used for earlier measurements of the excitation functions.[1] A bremsstrahlung beam was used to bombard a beryllium oxide target and the high-energy end-point region of the emitted proton spectrum was measured with a magnetic spectrometer. Photoprotons from $^9Be$ do not appear in this region because the $Q$ value and recoil energy are both larger for the $(\gamma,p)$ reaction on $^9Be$ than on $^{16}O$.

The principal change between the earlier work and that reported here and in Ref. 3 is the use of the One Hundred Inch Proton Spectrometer (OHIPS) to detect the protons in the present experiment. The apparatus and procedures are summarized below; further details can be found in Ref. 7.

The photon beam was generated by passing an electron beam through a 0.04 radiation-length tungsten radiator.

 

The resulting bremsstrahlung and the residual electron beam than impinged on a BeO target which was viewed by the OHIPS magnetic spectrometer. The radiator was located 15 cm upstream of the BeO target during all but the smallest angle measurements, in which case the separation was increased to 19 cm to ensure that the spectrometer did not view the radiator.

The target thickness was increased from 294 to 512 mg/cm$^2$ as the photon energy was raised. In this way the average proton energy loss in the target was kept approximately constant and made a contribution to the overall energy resolution of about 1.4 MeV full width at half maximum (FWHM).

The OHIPS magnetic spectrometer is a QQD design with point-to-point optics and a vertical bend plane. The angular acceptance is defined by an elliptical aperture, with a maximum scattering angle acceptance of $\pm 3°$ and maximum out-of-plane acceptance of $\pm 1°$, yielding a total solid angle of 3.8 msr. Focal plane drift chambers determined the trajectory of each event. Position and angle in the bend plane were used to calculate the momentum of each proton, and position and angle perpendicular to the bend plane were used to reject background events. Up to four plastic scintillators were mounted behind the focal plane as trigger counters. The pulse heights from these counters were used in the off-line analysis to identify proton events. The momentum calibration and quadrupole settings for OHIPS were determined using electron scattering measurements from a carbon target. Electrons with energy up to 630 MeV were focused onto the focal plane, with a typical momentum resolution $\Delta p/p$ of 0.15 percent FWHM.

With the radiator used in this experiment, typically two-thirds of the measured proton yield was produced by photodisintegration and one-third by electrodisintegration of $^{16}$O. In the analysis of the data the total effective photon flux incident on the target was calculated. The virtual photon spectrum was taken from Ref. 8 and the bremsstrahlung spectrum was calculated from the formulas in Ref. 9. Several measurements made with the radiator removed from the beam confirmed the reliability of these calculations.

A typical proton end-point spectrum is shown in Fig. 1. The contribution due to the population of the ground state of $^{15}$N is clearly distinguished from that due to the first three excited states in $^{15}$N, namely, the closely spaced $(\frac{1}{2}^+, \frac{5}{2}^+)$ doublet at 5.3 MeV and the 6.32-MeV $(\frac{3}{2}^-)$ state. Cross sections were extracted from the data by fitting four components to the measured proton spectra, corresponding to the excitation of the ground state, the 5.3 MeV doublet and the 6.32 MeV state, plus a uniform background. The shape of each component in the computed proton end-point spectrum was determined mainly by that of the incident photon spectrum, but the additional contributions from the proton energy loss in the target, the electron-beam energy resolution, and the spectrometer resolution were folded in, and together produced an additional contribution of 1.7 MeV FWHM to the proton energy resolution. For this reason the 5.3 and 6.32 MeV levels were not resolved. Only the ground-state cross sections and the summed cross sections for the first three excited states are reported in this paper.

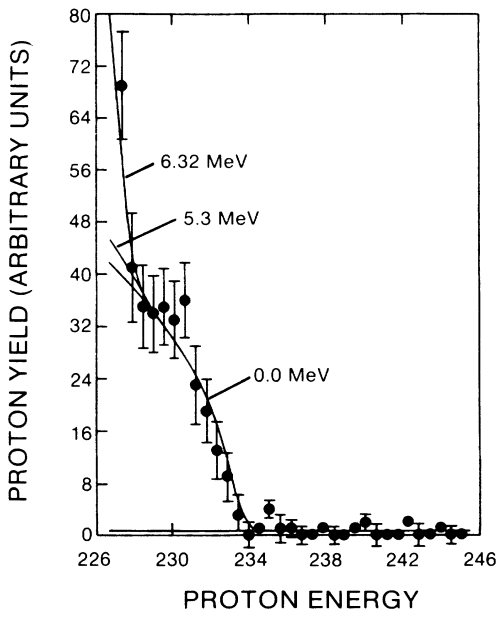


FIG. 1. Proton spectrum measured at 60° using photons having an endpoint energy of 257 MeV. The contributions to the fit due to a flat background, and the excitation of the $^{15}$N ground state, the 5.3-MeV doublet, and the 6.32-MeV excited state are indicated.

The resulting differential cross sections are displayed in Figs. 2 and 3 and are listed in Table I. The cross-section uncertainties shown there are statistical in origin. In addition to these one should include a systematic uncertainty of $\pm 7.4\%$ due to the contributions listed in Table II. In the regions where the measurements overlap, the present data are in good agreement with the data in Ref. 1.

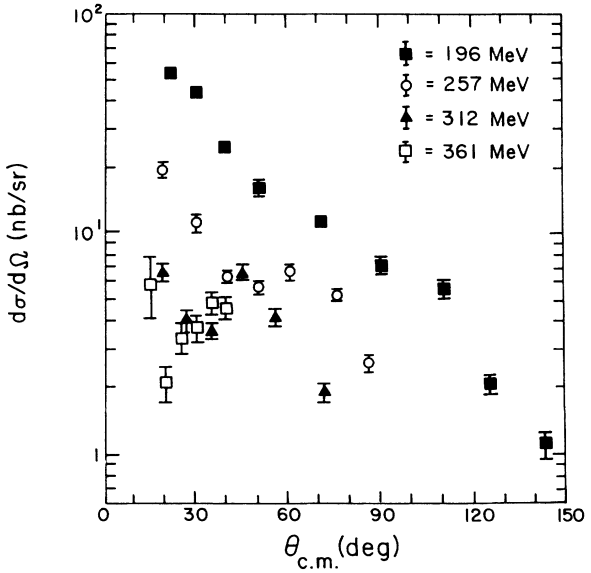


FIG. 2. Center-of-mass differential cross sections for the reaction $^{16}$O$(\gamma,p_0)^{15}$N at laboratory photon energies of 196 MeV (solid squares), 257 MeV (open circles), 312 MeV (triangles), and 361 MeV (open squares).

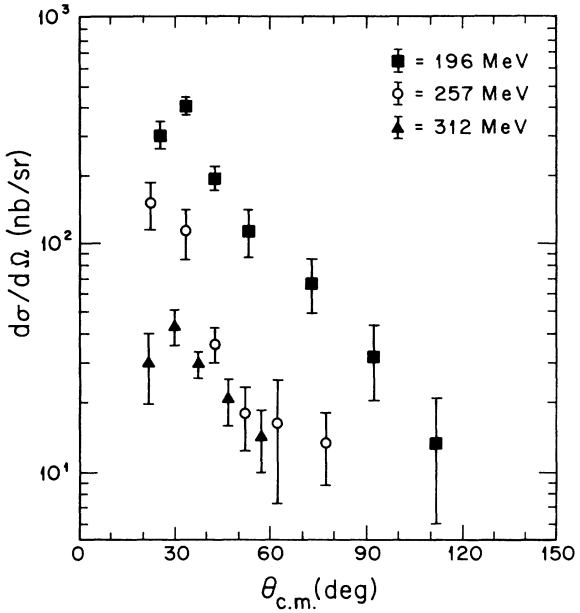


FIG. 3. Sum of the center-of-mass differential cross sections for populating the first three excited states in the reaction $^{16}O(\gamma,p_{1-3})^{15}N$ at photon energies of 196 MeV (squares), 257 MeV (open circles), and 312 MeV (triangles).

## III. DISCUSSION OF RESULTS

### A. Ground-state cross sections

Earlier measurements[10] of the $^{16}O(\gamma,p_0)$ angular distribution at photon energies up to 100 MeV showed a smoothly varying distribution, which became more forward peaked with increasing photon energy. This trend is continued in the present data for $E_\gamma = 196$ MeV, in which the cross section falls sharply with increasing proton angle. At the higher photon energies there is an additional systematic trend; the small inflection at $\theta_p \simeq 80°$ in the 196-MeV angular distribution becomes more pronounced and moves to more forward angles as the photon energy increases, ending as a deep minimum at 20° in the 361-MeV data. In terms of the momentum mismatch this feature in the cross section occurs at about the same value, $q \simeq 530$ MeV/$c$, at all photon energies and its origin is presumably the same as that of the changes previously observed[1] in the slopes of the 45°, 90°, and 135° excitation functions in this region of $q$. These systematic trends are compared below with those predicted by four theoretical calculations; the comparison could provide information on the contributions of different reaction mechanisms, since their varying relative importance is responsible for the systematic trends in the predictions.

Comparison is made first with the single-nucleon quasifree knockout (QFK) mechanism. In this mechanism the momentum mismatch, which has values 400–750 MeV/$c$ in the kinematic range of the present experiment, is provided by the initial momentum of the struck nucleon (with some momentum averaging and a shift in the mean mismatch momentum produced by the final-state optical potential). Since these values are far in excess of the Fermi momentum one does not expect the QFK amplitudes to be important at the upper end of the momentum mismatch range. The QFK calculations were carried out in a nonrelativistic framework using the distorted-wave impulse approximation[3,7,11] and both the electric and magnetic interaction terms were included. The final-state wave functions were generated in a central potential having a Saxon-Woods shape with radius parameter equal to

TABLE I. Center-of-mass differential cross sections for populating the ground state and excited states of $^{15}N$ in the $^{16}O(\gamma,p)$ reaction. Some of these data were reported in preliminary form in Ref. 3. Only statistical uncertainties are given.

| $E_\gamma$ lab (MeV) | c.m. angle (deg) | 0.0 MeV (nb/sr) | 5.3 + 6.32 MeV (nb/sr) |
|---|---|---|---|
| 196 | 22.1 | 53.6±2.7 | 304±41 |
| | 30.6 | 43.5±1.9 | 409±35 |
| | 40.3 | 24.4±1.6 | 195±24 |
| | 51.5 | 15.9±1.4 | 113±28 |
| | 71.3 | 11.1±0.70 | 66±18 |
| | 91.2 | 7.17±0.65 | 32±12 |
| | 111.3 | 5.62±0.53 | 13.3±7.4 |
| | 126.1 | 2.07±0.21 | |
| | 143.8 | 1.11±0.17 | |
| 257 | 19.5 | 19.4±1.5 | 150±37 |
| | 30.8 | 11.1±1.1 | 112±29 |
| | 41.1 | 6.35±0.47 | 35.9±6.4 |
| | 51.3 | 5.67±0.43 | 17.7±5.5 |
| | 61.4 | 6.62±0.56 | 16.1±8.9 |
| | 76.6 | 5.19±0.33 | 13.2±4.6 |
| | 86.6 | 2.58±0.24 | |
| 312 | 19.6 | 6.61±0.60 | 29.7±10.3 |
| | 27.6 | 4.02±0.41 | 43.0±7.7 |
| | 36.0 | 3.60±0.28 | 29.3±4.0 |
| | 45.8 | 6.66±0.44 | 20.4±4.7 |
| | 56.5 | 4.17±0.36 | 14.0±4.2 |
| | 72.4 | 1.88±0.19 | |
| 361 | 15.6 | 5.8±1.8 | |
| | 20.7 | 2.07±0.40 | |
| | 26.1 | 3.34±0.53 | |
| | 31.0 | 3.69±0.52 | |
| | 36.1 | 4.78±0.55 | |
| | 41.3 | 4.53±0.59 | |

TABLE II. Contributions to the systematic uncertainty in the absolute cross section (in percent).

| | |
|---|---|
| Solid angle | 0.5 |
| Beam-current integration | 1.0 |
| Real-photon spectrum | 5.0 |
| Virtual-photon spectrum | 4.0 |
| Electron-beam and spectrometer-energy calibration | 1.0 |
| Spectrometer dispersion | 0.7 |
| Dead-time corrections | 1.0 |
| Target thickness | 1.0 |
| Radiator thickness | 0.3 |
| Nuclear interactions in detectors | 3.0 |
| Total (in quadrature) | 7.4 |

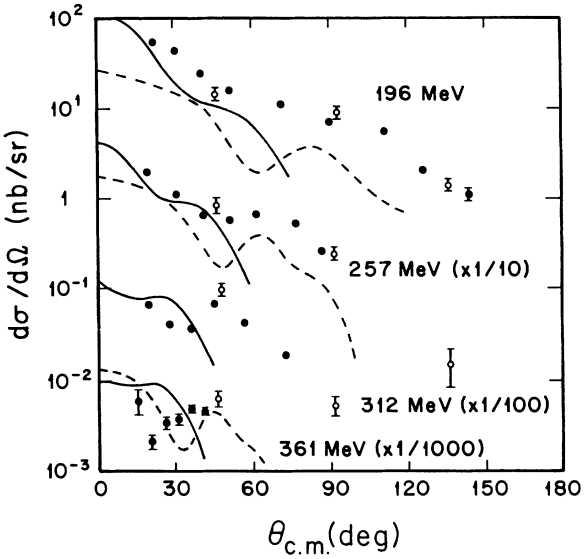


FIG. 4. The present data for the ground-state transition (solid circles) are plotted with data at comparable energies from Ref. 1 (open circles). The theoretical curves are the results of DWIA calculations using Elton and Swift (solid), and Negele finite-range (dashed) wave functions.

1.3 fm and diffusness equal to 0.65 fm. Optical potential depths were estimated[11] from the compilation of Passatore.[12] Real and imaginary potential depths of 7 and 10 MeV, respectively, were used for the calculations at $E_\gamma = 312$ MeV. These values are typical of those used for the other energies as well.

Calculations were carried out for two initial bound-state $p_{1/2}$ wave functions in $^{16}$O which differ markedly in the high-momentum region to which the present data are sensitive. One wave function was computed using the Elton-Swift bound-state potential[13] and the other was taken from the density-dependent Hartree-Fock calculations of Negele.[14] The latter wave function is known[15] to contain considerably more high-momentum components and also has its first minimum at a smaller value of nucleon momentum. The consequences of both differences can be identified in the results of the QFK calculations which are shown in Fig. 4. Both wave functions led to $(\gamma,p_0)$ cross sections which lie well below the $^{16}$O data over much of the measured range of photon energies and proton angles. The cross sections also have a dependence on $E_\gamma$ and $\theta_p$ which is qualitatively different from the data, although the Negele wave function is significantly better in this respect (having a minimum at more nearly the correct momentum). The comparison corroborates the conclusion of the earlier work[1] on $^{16}$O$(\gamma,p_0)$ that two-nucleon mechanisms play the main role at intermediate energies, although the one-nucleon mechanism may still make an important contribution. The striking differences between the predictions made with different bound-state wave functions emphasize the difficulty of estimating the QFK contribution because of its great sensitivity to the poorly known high-momentum components of the wave function.

Another calculation has been carried out within the QFK framework by Ryckebusch *et al.*[16] These authors use initial- and final-state wave functions calculated in a self-consistent way by the Hartree-Fock procedure using the Skyrme SkE2 effective interaction, and thus they avoid the criticism of using nonorthogonal wave functions for the initial and final states. The bound-state wave function also has more high-momentum components than the standard shell model forms, which are unrealistic in this respect. Ryckebusch *et al.* also ensure current conservation in their calculation, at the single-particle level, by choosing an appropriate form for the transition operators. Their results are in better agreement with the earlier $^{16}$O$(\gamma,p_0)$ data[1] than any of the other available calculations. At $E_\gamma = 196$ MeV, the only photon energy for which they have calculated the angular distribution, the agreement with the present data is reasonably good except at the forward angles where the cross sections are greatly overestimated. The cause of this disagreement is an overestimation of the magnetic QFK terms in the calculation, an effect which is also evident at higher photon energies in the results of Gari and Hebach[5] discussed below. In their calculations for $E_\gamma < 100$ MeV Ryckebusch *et al.* include random phase approximation (RPA) correlations in the nuclear wave functions. Although the predictions for the $(\gamma,n)$ reaction are altered dramatically when these correlations are included, the $(\gamma,p)$ predictions are less affected and it is argued that their neglect in the higher-energy calculations is not serious.

While the success of the Ryckebusch *et al.* calculation is encouraging, it is not clear that the QFK mechanism alone is responsible. Nonlocal effects are included in the calculation by the use the Skyrme interaction which has a strong momentum dependence, and this may simulate the effect of two-nucleon processes.

Two-body mechanisms in the $(\gamma,p_0)$ reaction have been investigated by several authors.[4–6] The calculation by Londergan and Nixon[4] (LN) includes in addition to QFK one of the possible two-nucleon mechanisms, the excitation of the $\Delta(1232)$ isobar in the intermediate state. Since the $\Delta$ coupling constants and form factors in their microscopic calculation are taken from experiment, there is little freedom in their results. LN find that the $\Delta$-excitation mechanism becomes dominant at $E_\gamma \gtrsim 200$ MeV and they predict a deep minimum in the cross section in the region where QFK and $\Delta$ excitation have similar amplitudes. This dip is responsible for the sharp fall at the most forward angles in the 210 MeV angular distribution predicted by LN. It is not seen in the 196 MeV data as shown in Fig. 5. At $E_\gamma = 300$ MeV where the $\Delta$-excitation amplitude dominates their result, LN obtain an angular distribution smoothly falling with angle. By contrast the 312-MeV data show a sharp minimum and the predicted forward-angle cross sections are a factor of 10 too large. The uncertainties in the QFK contributions that were referred to above could be a source of some of these discrepancies. A better treatment of final-state interactions would also tend to smooth out the sharp structure in the predicted cross sections. However, the lack of a consistent treatment of other two-nucleon mechanisms

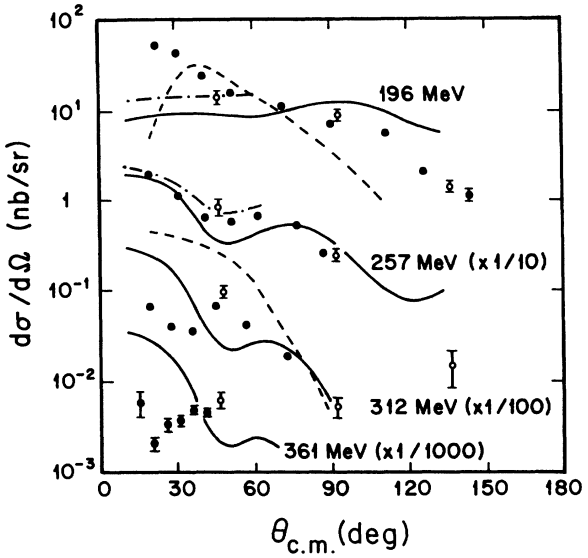


FIG. 5. The present data for the ground-state transition (solid circles) are plotted with data at comparable energies from Ref. 1 (open circles). The theoretical curves by Gari and Hebach for $E_\gamma = 200$, 260, 320, and 360 MeV (solid, without Δ; dotted-dashed, with Δ) and Londergan and Nixon (dashed) are explained in the text.

is a still more basic deficiency of the LN calculation. This criticism is implicit in the results obtained by Gari and Hebach,[5] who find that Δ excitation is by no means the most important two-nucleon mechanism, and who also make specific criticisms about the details of the LN treatment.

The calculation by Gari and Hebach[5] (GH) referred to above attempts to include all two-nucleon mechanisms other than Δ excitation. The GH formalism avoids a separate microscopic treatment of each contributing diagram by using the restrictions imposed by current conservation to relate the two-nucleon amplitudes to the residual *N-N* potential. In the GH evaluation these electric two-nucleon amplitudes are loosely subdivided into meson exchange current (MEC) and initial- and final-state nucleon correlation terms. These contributions are of comparable magnitude at $E_\gamma = 150$ MeV and the correlation terms becomes steadily less important at higher energies. The structure which appears in the results depicted in Fig. 5 is produced by the changing relative importance of the QFK terms and their interference with the MEC terms. At $E_\gamma = 200$ MeV GH find a strong cancellation between the QFK and MEC amplitudes, which reduces the cross section at angles up to $\theta_p = 80°$ and is responsible for the very poor agreement with data shown in Fig. 5. At backward angles corresponding to large values of the momentum mismatch, $q \geq 550$ MeV/$c$, the MEC terms do produce most of the cross section as expected but they are too large and exceed the data. At the higher photon energies GH find a still larger relative contribution from the QFK mechanism, specifically from the magnetic terms. This contribution dominates at forward angles and at the two highest photon energies it produces a forward-peaked cross section far above the data, so that one is led to regard the agreement with the 257-MeV data as fortuitous. At larger angles the GH predictions show a minimum at about 50 deg which is due to cancellation between the QFK and MEC amplitudes, followed by a second peak region in which the two-nucleon mechanism provides effectively all of the cross section. The data show a somewhat similar behavior but the minimum shifts to smaller angles as the photon energy is increased. Even if the interpretation of GH is basically correct one must conclude that both the magnitude and $E_\gamma$ dependence of the QFK and MEC amplitudes which they obtain are incorrect. The parametrizations chosen by GH to describe the residual *N-N* potential and the nucleon final-state potential have been questioned previously.[1] The present results again suggest that a reexamination is needed.

A final question about the GH treatment must lie with the absence of a full treatment of the Δ-excitation mechanism. GH have estimated the Δ-excitation contributions at the two lower photon energies for angles up to 60°. As shown in Fig. 5 they find a significant but not major increase in the cross section. However, in these regions the QFK contributions are still playing a large role and the photon energy is below the Δ resonance. It seems not improbable that, as suggested by LN, Δ excitation plays a major role at somewhat higher energies.

### B. Excited-state cross sections

In the present measurements the first few excited levels in $^{15}N$ were well resolved from the ground state but not from each other and only the summed cross section to the 6.32 MeV state with spin and parity $\frac{3}{2}^-$ and the 5.3-MeV $\frac{5}{2}^+, \frac{1}{2}^+$ doublet was obtained.

Since no theoretical estimates have been made for the positive parity excitations a detailed analysis of the present data is not possible. However, two features of the data are noteworthy. As seen in Fig. 3, the excited-state angular distributions do not show the sharp dip and second maximum that is evident in the higher-energy ground-state data. This indicates either that the angular distribution to the $\frac{3}{2}^-$ state is qualitatively different from that to the $\frac{1}{2}^-$ state or that there is a large contribution from the positive parity states. Strong population of the positive parity states might be expected in the region where two-nucleon amplitudes dominate since the wave functions for these states have larger two-hole one-particle components than do the negative parity states.[17] Moreover, this would be expected to produce an angular distribution quite different from that for the negative parity excitation. A strong excitation of the positive parity states could thus produce an angular distribution of the summed cross section that is featureless as observed.

The summed strength of the excited-state transitions is larger than that of the ground state by a factor of 3–10, depending on photon energy and scattering angle (see Table I and Ref. 1). This ratio seems large if one assumes that the measured cross section is mostly to the negative parity state at 6.32 MeV. The spectroscopic factors predict a ratio of 2 in that case, although more realistic cal-

culations in which the difference between the $1p_{1/2}$ and $1p_{3/2}$ wavefunctions is taken into account can explain ratios larger than 2 between the population of the negative parity states.[1,7] Clearly, high-resolution data on the excited-state transitions might provide a valuable pointer to the relative importance of QFK and two-nucleon mechanisms.

## IV. SUMMARY

The first detailed angular distributions for the $(\gamma,p)$ reaction at intermediate energies on an $A>4$ nucleus have been presented. Sharp structure develops in the angular distribution of the reaction $^{16}O(\gamma,p_0)^{15}N$ as the photon energy is raised from 196 to 361 MeV. A deep minimum followed by a second maximum is observed at the higher energies. The summed cross sections for the first three excited states in $^{15}N$ do not exhibit this structure. Quasifree knock-out calculations cannot account for the measured dependence on scattering angle and photon energy and the predicted cross sections are generally too small at large angles, indicating that two-nucleon mechanisms are important.

Calculations by Londergan and Nixon[4] and Gari and Hebach[5] which include two-nucleon mechanisms do obtain larger cross sections. However, neither calculation provides even a qualitatively satisfactory fit to the angular distribution data and it appears that relative magnitudes of the one- and two-nucleon contributions are incorrect in both treatments. A recent RPA calculation by Ryckebusch *et al.*[16] gives more promising results at the lowest photon energy measured, but it remains to be seen if this will be repeated at the higher energies. A complete theoretical treatment, which includes all the one- and two-nucleon mechanisms in a consistent way, is much needed.

Further experiments would also be of value as the angular range of the present measurements is very limited at the highest photon energies. Measurements for another nucleus would also be instructive. For example, in $^{40}Ca$ the existing excitation-function measurements[2] show more indications of structure than were seen in the comparable results[1] for $^{16}O$. Especially valuable would be comprehensive data for the $(\gamma,n_0)$ reaction in the energy range $E_\gamma>100$ MeV since a comparison with $(\gamma,p_0)$ results would give a straightforward measure of the importance of the convection-current QFK terms in the latter reaction.

## ACKNOWLEDGMENTS

We wish to thank W. K. Mize for his assistance in the data reduction phase of the experiment. This work was supported by the U.S. Department of Energy, the National Science Foundation, the U.K. Science and Engineering Research council, and Hughes Research Laboratories.

---

*Present address: Pichiney Research Center, CRV, BP27, 38340, Voreppe, France.

[1]M. J. Leitch *et al.*, Phys. Rev. C **31**, 1633 (1985).
[2]M. J. Leitch *et al.*, Phys. Rev. C **33**, 1511 (1986).
[3]R. S. Turley *et al.*, Phys. Lett. **157B**, 19 (1985).
[4]J. T. Londergan and G. D. Nixon, Phys. Rev. C **19**, 998 (1979).
[5]M. Gari and H. Hebach, Phys. Rep. **72**, 1 (1981).
[6]B. Schock, Phys. Rev. Lett. **41**, 80 (1978).
[7]R. S. Turley, Ph.D. thesis, Massachusetts Institute of Technology, 1984.
[8]L. Tiator and L. E. Wright, Comput. Phys. Commun. **28**, 265 (1983).
[9]J. L. Matthews and R. O. Owens, Nucl. Instrum. Methods **111**, 157 (1973).
[10]D. J. S. Findlay and R. O. Owens, Nucl. Phys. **A279**, 385 (1977).
[11]Douglas J. Gibson, Ph.D. thesis, University of Glasgow, 1979.
[12]G. Passatore, Nucl. Phys. **A248**, 509 (1975).
[13]L. R. B. Elton and A. Swift, Nucl. Phys. **94**, 52 (1966).
[14]J. W. Negele, Phys. Rev. C **1**, 1260 (1970).
[15]D. J. S. Findlay *et al.*, Phys. Lett. **74B**, 305 (1978).
[16]J. Ryckebusch *et al.*, Phys. Lett. B **194**, 453 (1987).
[17]E. C. Halbert and J. B. French, Phys. Rev. **105**, 1563 (1957).